



## Second-order advantage with excitation–emission photoinduced fluorimetry for the determination of the antiepileptic carbamazepine in environmental waters

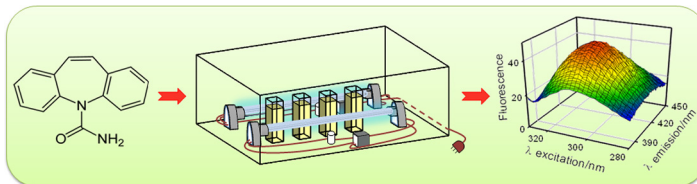
Valeria A. Lozano, Graciela M. Escandar\*

*Instituto de Química Rosario (CONICET-UNR), Facultad de Ciencias Bioquímicas y Farmacéuticas, Universidad Nacional de Rosario, Suipacha 531, 2000 Rosario, Argentina*

### HIGHLIGHTS

- A simple and safe method for the emerging contaminant carbamazepine is developed.
- MCR-ALS algorithm allows us the quantification in very interfering media.
- Determination is accomplished in natural waters using green-chemistry principles.

### GRAPHICAL ABSTRACT



### ARTICLE INFO

#### Article history:

Received 4 March 2013

Received in revised form 8 April 2013

Accepted 10 April 2013

Available online 17 April 2013

#### Keywords:

Photoinduced fluorescence  
Multivariate calibration  
Carbamazepine

### ABSTRACT

A photochemically induced fluorescence system combined with second-order chemometric analysis for the determination of the anticonvulsant carbamazepine (CBZ) is presented. CBZ is a widely used drug for the treatment of epilepsy and is included in the group of emerging contaminant present in the aquatic environment. CBZ is not fluorescent in solution but can be converted into a fluorescent compound through a photochemical reaction in a strong acid medium. The determination is carried out by measuring excitation–emission photoinduced fluorescence matrices of the products formed upon ultraviolet light irradiation in a laboratory-constructed reactor constituted by two simple 4 W germicidal tubes. Working conditions related to both the reaction medium and the photoreactor geometry are optimized by an experimental design. The developed approach enabled the determination of CBZ at trace levels without the necessity of applying separation steps, and in the presence of uncalibrated interferences which also display photoinduced fluorescence and may be potentially present in the investigated samples. Different second-order algorithms were tested and successful resolution was achieved using multivariate curve resolution-alternating least-squares (MCR-ALS). The study is employed for the discussion of the scopes and yields of each of the applied second-order chemometric tools. The quality of the proposed method is probed through the determination of the studied emerging pollutant in both environmental and drinking water samples. After a pre-concentration step on a C18 membrane using 50.0 mL of real water samples, a prediction relative error of 2% and limits of detection and quantification of 0.2 and 0.6 ng mL<sup>-1</sup> were respectively obtained.

© 2013 Elsevier B.V. All rights reserved.

**Abbreviations:** CBZ, carbamazepine;  $C_{CBZ}$ , concentration of carbamazepine;  $C_{HCl}$ , concentration of hydrochloric acid; EEPIMs, excitation–emission photoinduced fluorescence matrices; EJCR, elliptical joint confidence region; EU, European Union; IT, irradiation time; LD, distance between the lamps; LOD, limit of detection; LOQ, limit of quantification; MCR-ALS, multivariate curve resolution-alternating least-squares; N-PLS/RBL, multidimensional partial least-squares/residual bilinearization; PARAFAC, parallel factor analysis; PMT, photomultiplier tube; R, correlation coefficient; SPE, solid-phase extraction; SVD, singular value decomposition; U-PLS/RBL, unfolded partial least-squares/residual bilinearization.

\* Corresponding author. Tel.: +54 341 4372704; fax: +54 341 4372704.

E-mail addresses: [escandar@iquir-conicet.gov.ar](mailto:escandar@iquir-conicet.gov.ar), [gmescandar@hotmail.com](mailto:gmescandar@hotmail.com) (G.M. Escandar).



## 1. Introduction

Carbamazepine (CBZ), 5H-dibenzo[b,f]azepine-5-carboxamide (Fig. 1) is an anticonvulsant drug widely used for the treatment of epilepsy and psychiatric diseases [1], and is included in the group of emerging contaminants [2]. This pharmaceutical pollutant is of particular concern because of its important toxicological and pharmacological effects in mammals, humans and the aquatic environment [3–6], in addition to the harmful consequences produced by its major photoproduct, acridine [7,8].

Environmental studies have demonstrated that CBZ is one of the most frequently detected pharmaceutical in sewage-treatment plant effluents, river water and drinking water [9,10]. A field study of occurrence and fate of CBZ and other five pharmaceuticals in surface waters of Switzerland concluded that CBZ reached concentrations of 0.4 and 0.95 ng mL<sup>-1</sup> in river and wastewater treatment plant effluents, respectively [11]. An European Union (EU) monitoring study for organic compounds in rivers and streams across Europe indicated that CBZ is one of the most frequently detected compound (95%), with an average concentration of 0.25 ng mL<sup>-1</sup> and maximum concentrations of about 11 ng mL<sup>-1</sup> [12]. A recent study related to the occurrence of polar organic pollutants in EU ground waters included CBZ in the list of most frequently found pharmaceuticals (42.1%), with a maximum concentration of 0.39 ng mL<sup>-1</sup> [13].

CBZ seems to be persistent in the environment, therefore qualifying as a suitable marker for anthropogenic influences on the aquatic environment [14]. The determination of CBZ and atrazine was employed as a target analysis for tracers of organic contamination in drinking and surface waters, resulting in a useful tool to prioritize samples which should be further screened for suspect contaminants [15].

Very recently, during the analysis of selected pharmaceuticals in fish and surface waters directly affected by irrigation with reclaimed water, CBZ was consistently detected, with a significant bioaccumulation factor in mosquito fish [16].

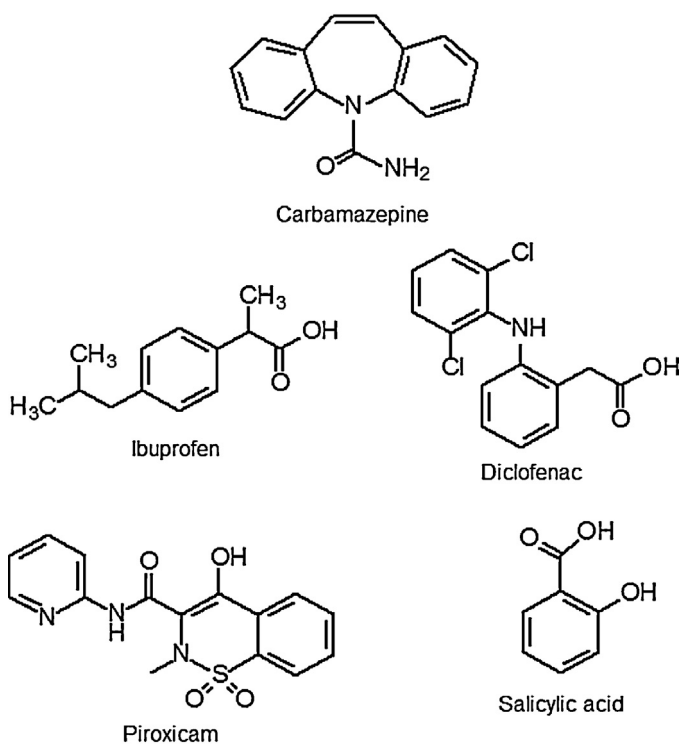


Fig. 1. Structure of carbamazepine and potential interferences.

Chromatographic methods are the most commonly applied ones for the determination of CBZ or its photodegradation products in different matrices [9–39], although spectrophotometric, mass spectrometric, electrochemical and capillary electrophoretic methods have also been proposed [40–47]. Since CBZ is not fluorescent in solution, fluorimetric methods for its determination have been developed in a nylon surface [48] or through the formation of fluorescent derivatives by oxidation with Ce(IV) [49,50], permanganate [51] and lead dioxide [52], or by photochemical reaction [53].

The determination of contaminants in complex samples brings the problem of the presence of interfering agents which must be removed, extending the analysis time and the experimental work. On the other hand, these separative steps frequently involve the use of organic solvents which are harmful to health and pollute the environment. In this regard, with the purpose of contributing with the protection of the environment and decreasing the health impact, there is a particular interest in developing methods for analytes of ecological concern complying with the principles of green analytical chemistry [54,55].

In this paper, we present a new and safe photochemically induced fluorescence system for the determination of CBZ in environmental water samples without involving organic solvents. An acidic solution of CBZ is irradiated with two germicidal UV lamps, and the concentration of the formed photoproducts is then spectrofluorimetrically determined in the presence of pharmaceuticals (or their photoproducts) usually detected in the aquatic environment, coupling excitation–emission photoinduced fluorescence matrices (EEPIFMs) to multivariate calibration. Four chemometric algorithms which achieve the second-order advantage, namely, parallel factor analysis (PARAFAC) [56] unfolded partial least-squares coupled to residual bilinearization (U-PLS/RBL) [57,58], multidimensional partial least-squares [59] coupled to residual bilinearization (N-PLS/RBL), and multivariate curve resolution-alternating least-squares (MCR-ALS) [60] were applied to process the EEPIFMs. Second-order advantage refers the capacity of certain second-order algorithms to predict concentrations of sample components in the presence of any number of unsuspected constituents [61,62]. Notable differences in the prediction capabilities of the employed algorithms were observed and discussed, and the feasibility of determining CBZ in natural water samples is demonstrated.

## 2. Experimental

### 2.1. Reagents and solutions

CBZ was obtained from Sigma (St. Louis, MO, USA). Methanol and hydrochloric acid were purchased from Merck (Darmstadt, Germany). Compounds tested as potential interferents were of analytical grade and were used as received. The stock solution of CBZ (530 µg mL<sup>-1</sup>) was prepared in methanol. From this solution, more diluted aqueous working solutions were obtained. Ultrapure Milli-Q water was used throughout the work.

### 2.2. Instrumentation

Fluorescence spectra were measured using an Aminco Bowman (Rochester, NY, USA) Series 2 luminescence spectrometer equipped with a 150 W xenon lamp. These spectra were obtained using excitation and emission wavelengths of 308 and 410 nm, respectively, and both the excitation and emission slit widths were of 8 nm using 1.00 cm quartz cells. The photomultiplier tube (PMT) sensitivity was fixed at 700 V and the temperature of the cell compartment was kept constant at 20 °C by circulating water from a thermostatted bath (Cole-Parmer, IL, USA).

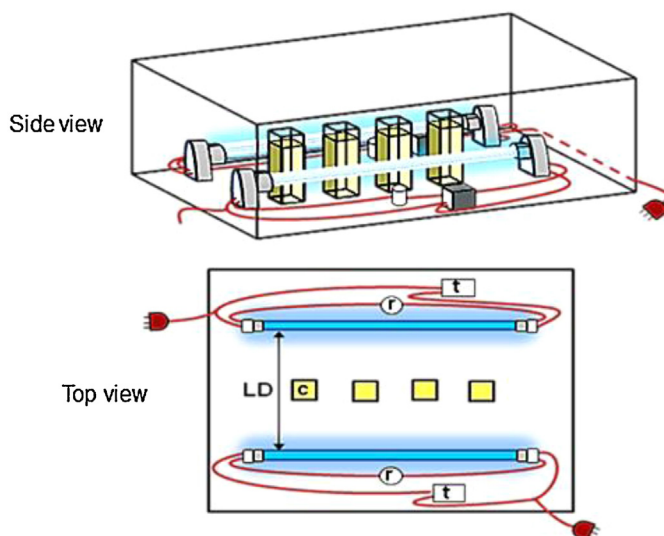


**Fig. 2.** Photoreactor. LD, distance between the lamps; C, quartz cells; r, reactance; t, transformer.

### 2.3. Procedure

The photodegradation reaction was carried out in a very simple reactor constructed in our laboratory, constituted by two germicidal tubes of 4 W (Fig. 2). Both the geometry of the photoreactor and the experimental conditions to reach the best signal were optimized (see below). EEPIMs were measured from 280 to 320 nm (each 2 nm) and from 380 to 450 nm (each 1 nm), respectively, and were then subjected to second-order data analysis.

### 2.4. Optimization of the parameters affecting the fluorescence signal

A five-level central composite design of 17 experiments was applied for investigating the influence of the three variables on the fluorescence intensity, with three replicates at the central point. These variables were the concentration of hydrochloric acid ( $C_{\text{HCl}}$ ), the irradiation time (IT) and the distance between the lamps (LD). The fluorescence intensity was recorded for each solution using 308 and 410 nm as excitation and emission wavelengths, respectively. The runs were carried out in a randomized sequence to minimize the effect of uncontrolled variables on the response. The resulting experimental matrix is detailed in Table 1, and the quadratic regression model selected to define the relationship between the response and the variables was:

$$F = b_0 + \sum_{i=1}^3 b_i x_i + \sum_{i=1}^3 b_{ii} x_i^2 + \sum_{i=1}^3 \sum_{j=i+1}^3 b_{ij} x_i x_j + e \quad (1)$$

where  $F$  is the response,  $x_i$  and  $x_j$  are the studied factors,  $b_0$ ,  $b_i$ ,  $b_{ii}$  and  $b_{ij}$  are the intercept, linear, quadratic and interaction coefficients, and  $e$  the model error.

### 2.5. Quantitative analysis

Preliminary experiments indicated that, under the established working conditions, linearity is held until  $61 \text{ ng mL}^{-1}$ , which was the limiting assayed concentration in subsequent analyses.

A calibration set of 9 samples was prepared, by duplicate, measuring appropriate aliquots of stock solution of CBZ into 2.00 mL calibrated flasks, evaporating the solvent with nitrogen and completing to the mark with  $2 \text{ mol L}^{-1}$  HCl. A validation set was similarly prepared employing concentrations different from those

**Table 1**  
Design generated for a central composite design and the obtained response values.

Run	$b_1 - C_{\text{HCl}}$ (M)	$b_2 - \text{IT}$ (min)	$b_3 - \text{LD}$ (cm)	$F$ (response)
1	1.50	1.00	6.00	5.8
2	1.50	30.00	6.00	24.7
3	2.50	7.00	8.00	16.7
4	3.00	16.00	6.00	32.6
5	2.50	25.00	3.50	25.4
6	0.30	16.00	6.00	14
7	1.50	16.00	10.00	26.5
8	1.50	16.00	6.00	31.8
9	0.50	7.00	8.00	15.4
10	0.50	25.00	3.50	6.4
11	0.50	25.00	8.00	21.8
12	1.50	16.00	6.00	33.6
13	2.50	25.00	8.00	29.2
14	1.50	16.00	2.00	23.6
15	1.50	16.00	6.00	33.7
16	2.50	7.00	3.50	24.7
17	0.50	7.00	3.50	6.3

$C_{\text{HCl}}$ , concentration of hydrochloric acid; IT, irradiation time; LD, distance between the lamps.

used for calibration and following a random design. With the purpose of evaluating the proposed strategy in the presence of these interferent agents, 20 additional test samples containing random concentrations of CBZ and these foreign compounds were prepared. The interferents were evaluated at the following concentration ranges: 0–5600, 0–1200, 1–9, and 0–5000  $\text{ng mL}^{-1}$  for ibuprofen, diclofenac, piroxicam, and salicylic acid, respectively. The maximum level of each evaluated interference was selected in order to avoid the saturation of the fluorescence signal. Taking into account that the highest CBZ concentration was about  $60 \text{ ng mL}^{-1}$ , with the exception of piroxicam, each interferent agent was between 16 and 90 times more concentrated than the analyte.

### 2.6. Real water samples

All investigated water samples were prepared by spiking them with CBZ at three different concentrations, obtaining levels between  $0.4$  and  $5.5 \text{ ng mL}^{-1}$ . Tap water from Rosario city (Santa Fe, Argentina) and underground water from Funes and Venado Tuerto cities (Santa Fe, Argentina) samples were used as received. The Paraná River sample was collected near Rosario city, and after spiking it with CBZ, it was filtered through a filter paper to remove suspended solid materials. In order to improve the sensitivity of water analysis, a solid-phase extraction (SPE) procedure with C18 membranes was applied. Prior to sample application, each membrane was conditioned with  $500 \mu\text{L}$  of methanol. Positive pressure was used to force the water sample through the membrane. For concentrations of CBZ at sub-part-per-billion levels,  $50.0 \text{ mL}$  of sample was employed, while a volume of  $10.0 \text{ mL}$  was used for the remaining samples. Following the extraction, the disk was dried by forcing air through it using a  $25 \text{ mL}$  syringe. Then, the retained CBZ was eluted with  $500 \mu\text{L}$  of methanol and the liquid was collected in a  $2.00 \text{ mL}$  volumetric flask. After evaporation of the solvent with nitrogen, the residue was reconstituted to the mark with  $2 \text{ mol L}^{-1}$  HCl. Thus, the pre-concentration factors were 25 and 5 for samples with sub-part-per-billion and part-per-billion concentrations, respectively. Then, the procedure described above was performed.

### 2.7. Software

The experimental design and optimization were carried out using Design Expert 6.0 (Stat-Ease Inc.). The employed chemometric algorithms were written in MATLAB 7.6 [63]. PARAFAC, U- and N-PLS/RBL were implemented using the graphical interface of the MVC2 toolbox, which can be freely downloaded from the

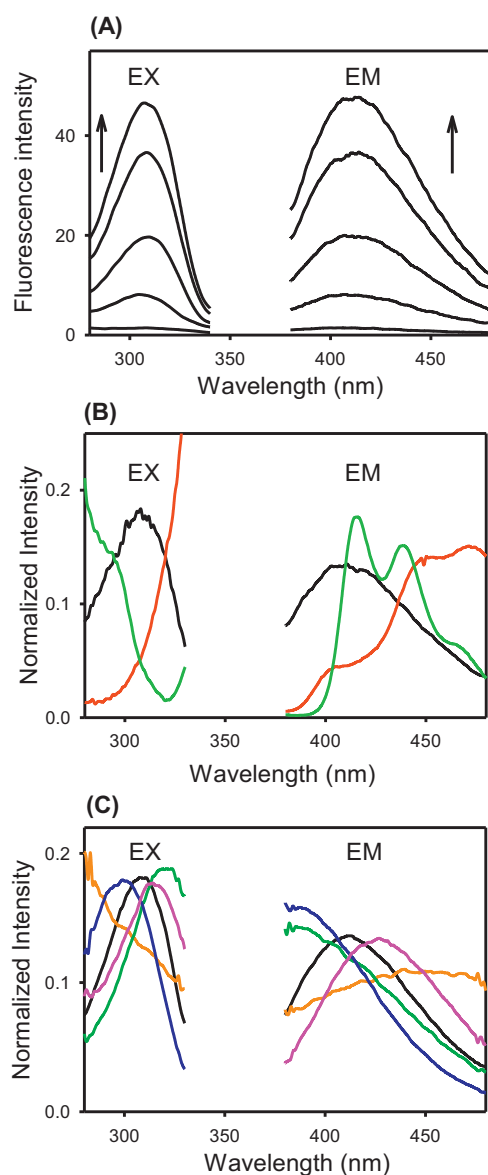


**Fig. 3.** (A) Excitation and emission fluorescence spectra of CBZ photoproducts (initial  $C_{CBZ} = 0, 10.1, 25.3, 48.0$ , and  $60.0 \text{ ng mL}^{-1}$ ). (B) Normalized excitation and emission fluorescence spectra of CBZ photoproducts (black line), acridine (red line) and acridone (light green line). (C) Normalized excitation and emission fluorescence spectra of CBZ (black line), ibuprofen (orange line), diclofenac (green line), piroxicam (blue line), and salicylic acid (pink line) after irradiation under the used experimental condition. (For interpretation of the references to color in this figure legend, the reader is referred to the web version of this article.)

web page [www.quir-conicet.gov.ar/descargas/mvc2.rar](http://www.quir-conicet.gov.ar/descargas/mvc2.rar). MCR-ALS is available in the Internet at <http://www.mcrals.info/>. Theoretical considerations of the applied algorithms can be found in the supplementary information.

### 3. Results and discussion

#### 3.1. Preliminary studies

As was previously indicated, CBZ does not display native fluorescence, but emission can be obtained upon UV irradiation under certain working conditions, indicating the formation of one or more emissive photoproducts (Fig. 3A). In the literature, different CBZ photoproducts have been reported depending on the employed experimental conditions.

**Table 2**  
Analysis of variance (ANOVA) for the selected quadratic model.<sup>a</sup>

Source	Sum of squares	DF	Mean square	F value	p > F
Model	1408.40	8	176.05	23.46	<0.0001
$b_1 - C_{HCl}$	511.89	1	511.89	68.22	<0.0001
$b_2 - IT$	151.89	1	151.89	20.24	0.020
$b_3 - LD$	58.01	1	58.01	7.73	0.0239
$b_{11}$	179.14	1	179.14	23.87	0.0012
$b_{22}$	464.96	1	464.96	61.978	<0.0001
$b_{33}$	88.71	1	88.71	11.82	0.0088
$b_{13}$	97.37	1	97.37	12.98	0.0070
$b_{23}$	45.05	1	45.05	6.00	0.0399
Lack of Fit					0.100

DF = degree of freedom;  $p$  = probability;  $R^2$  (coefficient of determination) = 0.959; Pred  $R^2$  (measures how well the model will predict the responses for a new experiment) = 0.794; Adeq precision (measures the signal to noise ratio) = 13.97.

<sup>a</sup> The term  $b_{12}$  was not significant ( $p > 0.05$ ) and was excluded of the analysis.

For example, acridine and acridone were the main identified photoproducts when an acid solution of CBZ was irradiated with a 1500 W arc xenon lamp during 30 min [64]. CBZ treatment with UV irradiation (17 W mercury lamp, 254 nm) in the presence of  $H_2O_2$  produced acridine, a series of acridine intermediates and small amounts of salicylic acid, catechol and anthranilic acid among the reaction products [65]. Chiron et al. studied the photodegradation of CBZ in artificial estuarine water, mimicking natural processes [7]. After evaluating different experimental conditions, it was concluded that besides acridine (the major photodegradation intermediate), 10-hydroxycarbamazepine, hydroxyacridine-9-carboxaldehyde, and acridone are also formed.

Under our working conditions, the obtained wide spectra with excitation and emission maxima at 308 and 410 nm, respectively, do not suggest a significant contribution of either acridine or acridone (Fig. 3B). However, regardless of the nature of the formed photoproducts, a linear relationship between the CBZ concentration and the obtained fluorescence intensity was corroborated and, therefore, a quantitative analysis could be properly developed.

#### 3.2. Optimization of the experimental conditions

Exploratory experiments showed that the type and concentration of acid used in the reaction medium, the time of sample irradiation and the distance between the reactor lamps (the sample is positioned equidistant between both lamps) had critical effects on the photochemically induced fluorescence. Although in some systems the presence of different organized media could sensitize photochemical reactions [66,67], in our working conditions selected surfactants (sodium dodecyl sulfate, hexadecyltrimethylammonium bromide, Triton X-100) and cyclodextrins ( $\beta$ -,  $\gamma$ -,  $\alpha$ - and 2-hydroxy-propyl- $\beta$  cyclodextrins) did not produce a significant signal improvement. On the other hand, deoxygenation of the medium with a flow of nitrogen did not improve the signal intensity.

As regards the acid employed, nitric, sulfuric and hydrochloric acids were checked. In the presence of nitric acid, signals were not detected, and the sulfuric acid background signal was significant. Hydrochloric acid produced the best signals and, therefore, it was selected for the subsequent experiments.

It was found that irradiation with two 4 W lamps, rather than using either one 4 W lamp or 8 W lamps, produced an efficient photodegradation reaction of CBZ. Besides, the distance between these lamps and the time of irradiation modified the signal. These factors were optimized using a surface response methodology. Table 2 displays the ANOVA results for the selected quadratic model, where it can be appreciated that the variables explain the data and indicate that the variable effect is significant at 95% confidence level.

The coefficients estimated for the mathematical model in terms of actual factors were: -40, 31, 2.3, 6.9, -5.2, -0.08, -0.48, -1.5 for intercept,  $C_{\text{HCl}}$ , IT, LD,  $(C_{\text{HCl}})^2$ ,  $(\text{IT})^2$ ,  $(\text{LD})^2$ ,  $C_{\text{HCl}} \times \text{LD}$  and  $\text{IT} \times \text{LD}$ , respectively.

The optimum values obtained for  $C_{\text{HCl}}$ , IT and LD were 2 mol L<sup>-1</sup>, 20 min and 6 cm, respectively. These conditions were used for the corresponding quantitative analysis.

It is important to point out that the geometry of the photoreactor (Fig. 2) allows the simultaneous irradiation of four solutions contained in the quartz cells. Thus, the time of irradiation is equivalent to 5 min per sample.

### 3.3. Quantitative analysis

The purpose of the present work is to determine CBZ in natural matrices where other concomitantly present compounds are potentially able to produce interference through either themselves or their fluorescent photoproducts when the sample is subjected to the irradiation protocol. Therefore, different pharmaceuticals selected from the list of organic micropollutants usually detected in the aquatic environment were checked as potential interferents, namely ibuprofen, diclofenac, piroxicam, salicylic acid, naproxen, ketoprofen and atenolol [11,68]. We found that, after irradiation, the excitation and emission spectra of the photoproducts of the first four compounds (Fig. 1) are significantly overlapped with those corresponding to CBZ ones, producing a severe interference (Fig. 3C). Thus, for improving the selectivity of the method, a second-order calibration applying algorithms which achieve the so-called second-order advantage was proposed.

Firstly, EEPIMs of CBZ photoproducts under optimal working conditions were recorded for calibration and validation samples (Fig. 4A), where only the studied analyte is present. These matrices were successfully resolved by usual second-order algorithms such as PARAFAC, U-PLS, N-PLS and MCR-ALS (data not shown). However, the results were different when test samples containing interferent agents were processed. Fig. 4B shows the three-dimensional plot of the EEPIM for a typical sample with interferences and the corresponding contour plot. The results obtained with different algorithms applied to these samples are discussed below.

#### 3.3.1. PARAFAC

The PARAFAC model allowed us to obtain physically interpretable profiles. The identification of the analyte was done with the aid of the estimated excitation and emission profiles, and comparing them with those for an irradiated standard CBZ solution. The number of components was selected by the so-called core consistency analysis [69], which consists in studying the structural model based on the data and the estimated parameters of gradually augmented models. A PARAFAC model is considered to be appropriate if incorporating an additional component does not improve the fit considerably [69]. The number of components also was analysed through the spectral profiles produced by the addition of a new component. If this addition generated repeated profiles, suggesting overfitting, this new component was discarded. The number of responsive components obtained using both procedures was two in validation samples and three in samples with interferences. In validation samples, the obtained number of components could be justified taking into account the presence of two different signals corresponding to CBZ and background signals. On the other hand, in test samples interferences are extracted as a single signal.

PARAFAC was initialized with the loadings giving the best fit after a small number of trial runs, selected from the comparison of the results provided by generalized rank annihilation and several random loadings [70].

Fig. 5A shows the prediction results corresponding to the application of PARAFAC to the 20 samples with interferences. As can be appreciated, the results are rather poor. This fact may be explained considering the significant spectral overlapping among the analyte and interferences, which precludes the successful decomposition of the second-order data [71]. The elliptical joint confidence region (EJCR, [72]) test for the slope and intercept of the found vs. nominal concentrations plot shows that the ideal point (1,0) lies outside the EJCR surface (Fig. 5F), also suggesting that PARAFAC is inappropriate for resolving the system under investigation.

#### 3.3.2. U- and N-PLS

In the cases of U- and N-PLS/RBL, the optimum number of factors for the calibration set applying the cross-validation method described by Haaland and Thomas [73] was also two. When these algorithms were applied to samples containing interferents, in addition to the latent variables estimated from the calibration set, they required the introduction of the RBL procedure with an additional number of components corresponding to the unexpected sample constituents. This number, estimated by suitable consideration of RBL residues [74], ranged from 1 to 2. Adding more unexpected components did not improve the fit. Apparently, PLS/RBL considers the profiles of the four interferences as additional one or two components, and is able to distinguish these combined signals from those of the analyte and the blank. Fig. 5B and C shows the prediction results corresponding to the application of U-PLS/RBL and N-PLS/RBL to the samples containing interferences. In these figures, some dispersion of the predictions with respect to the perfect fit lines is verified. While the corresponding ellipses include the theoretical (1,0) point (Fig. 5F), they show large (and undesirable) sizes. However, although these algorithms have some difficulty to solve the system under study, they are more flexible and render better results than PARAFAC.

#### 3.3.3. MCR-ALS

The MCR-ALS model decomposes an augmented data matrix, built by placing matrices for different samples adjacent to each other, in such a way that the augmentation mode is the one affected by the profile overlapping. As a result, the poor selectivity in the affected dimension is recovered in the augmented dimension. In the present system, since a significant overlapping between analyte and interferences is observed in the excitation and emission spectra, both modes of augmentation were checked. Therefore, two different data processing were performed: one of them comprised the building of augmented column-wise (emission spectral) data matrices containing the test sample data and the calibration data matrices, and the other one comprised the building of augmented row-wise (excitation spectral) data matrices, also containing the test and calibration data matrices.

Before starting resolution, the determination of the number of MCR components was estimated by applying singular value decomposition (SVD). Usually, the plot of singular values as a function of principal component number is visually inspected, locating a number for which the plot stabilizes. This number is initially employed for MCR-ALS analysis, and is afterwards refined (increased or decreased) until an appropriate solution is found, with a reasonable least-squares fit and physically recognizable profiles. Given the number of responsive components, their spectra were then obtained from the analysis of the so-called "purest" spectra, based on the SIMPLISMA methodology, a multivariate curve resolution algorithm which extracts the purest spectra of the mixture from a series of spectra of mixtures of varying composition [75]. The spectra provided by SIMPLISMA were suitable to perform the resolution and, therefore, it was not necessary to include reference spectra for the analyte as initial estimates for MCR-ALS. In the present system, the number of MCR components in both augmentation modes was

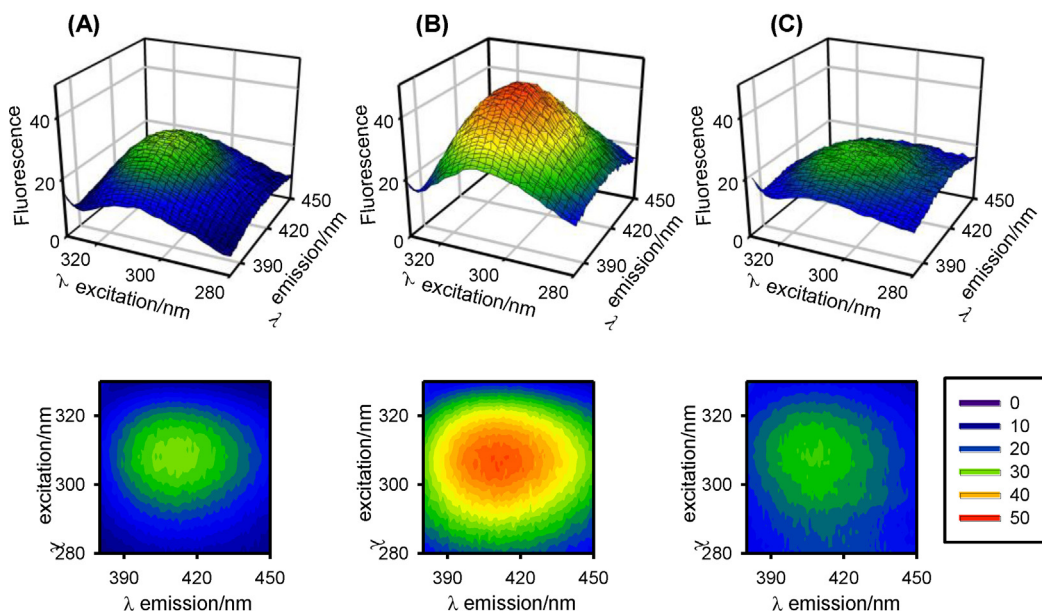


**Fig. 4.** Three-dimensional plots and the corresponding contour plots of excitation–emission photoinduced fluorescence matrices for (A) a validation sample containing  $48.0 \text{ ng mL}^{-1}$  CBZ, (B) a test sample containing  $56.0 \text{ ng mL}^{-1}$  CBZ,  $2000 \text{ ng mL}^{-1}$  ibuprofen,  $1500 \text{ ng mL}^{-1}$  salicylic acid,  $600 \text{ ng mL}^{-1}$  diclofenac and  $2 \text{ ng mL}^{-1}$  piroxicam, and (C) a spiked river sample after solid-phase extraction (original  $C_{\text{CBZ}} = 5.5 \text{ ng mL}^{-1}$ ).

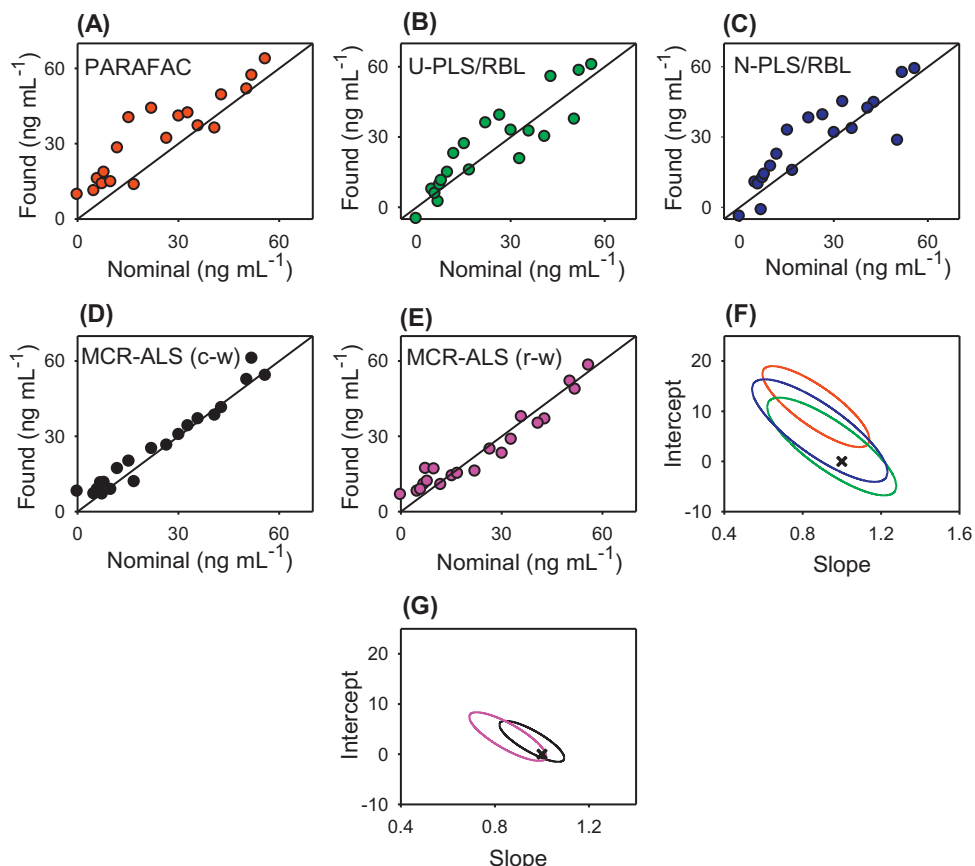


**Fig. 5.** Plots for CBZ predicted concentrations in samples with interferences (test samples) as a function of the nominal values using (A) PARAFAC, (B) U-PLS/RBL, (C) N-PLS/RBL, (D) MCR-ALS (column-wise augmentation), and (E) MCR-ALS (row-wise augmentation). Solid lines indicate the perfect fits. (F) Elliptical joint regions (at 95% confidence level) for slope and intercept of the regression of PARAFAC (red line), U-PLS/RBL (green line), and N-PLS/RBL (blue line). (G) Elliptical joint regions (at 95% confidence level) for slope and intercept of the regression of MCR-ALS using column-wise (black line) and row-wise (pink line) augmentations. Crosses in (F) and (G) mark the theoretical (intercept = 0, slope = 1) point. (For interpretation of the references to color in this figure legend, the reader is referred to the web version of this article.)

**Table 3**

Statistical results for CBZ using the proposed methodology and MCR-ALS (column-wise augmentation).

	Test samples <sup>a</sup>	Real water samples <sup>b</sup>	Real water samples <sup>c</sup>
LOD <sup>d</sup> (ng mL <sup>-1</sup> )	5	1	0.2
LOQ <sup>e</sup> (ng mL <sup>-1</sup> )	15	3	0.6
RMSEP <sup>f</sup> (ng mL <sup>-1</sup> )	4	0.4	0.1
REP <sup>g</sup> (%)	13	7	2

<sup>a</sup> Twenty samples containing ibuprofen, diclofenac, piroxicam, salicylic acid as interferents.

<sup>b</sup> Pre-concentration factor = 5 (the results refer to the original water sample before SPE).

<sup>c</sup> Pre-concentration factor = 25 (the results refer to the original water sample before SPE).

<sup>d</sup> LOD, limit of detection calculated according to Ref. [78].

<sup>e</sup> LOQ, limit of quantitation calculated as LOD × (10/3.3).

<sup>f</sup> RMSEP, root-mean-square error of prediction.

<sup>g</sup> REP, relative error of prediction.

three. Apparently, the algorithm combines the signals of interferents but perfectly distinguishes them from those belonging to the analyte and, as will be shown below, yields very good predictions.

During the iterative procedure leading to chemically recognizable solutions the constraint of non-negativity in both data modes was applied. The selected MCR convergence criterion was 0.1% (relative change in fit for successive iterations) and the maximum number of iterations was set to 1000. Convergence was achieved after less than 300 iterations in most of the evaluated samples. Further, the quality of the MCR-ALS recovered spectral profiles was evaluated using the criterion of similarity which involves a comparison, through the correlation coefficient (*R*) between the reference and evaluated spectrum [76]. The value of *R* found for CBZ photoproducts in the excitation and emission spectra were 0.9992 and 0.9997, respectively, corroborating the excellent quality of the MCR-ALS obtained results.

Fig. 5D and E shows the prediction results corresponding to the application of MCR-ALS to the same test samples described above using the column- and row-wise augmentation, respectively. As can be observed, in both cases the predictions are in good agreement with the corresponding nominal values, with the results of column-wise augmentation being slightly better. This fact could be ascribed to the better selectivity achieved through the excitation spectra. The EJCR test (Fig. 5G) corroborates that both ellipses have a small size and include the theoretically expected values of (1,0), demonstrating the accuracy of the used methodologies.

The statistical results are complemented with the values shown in Table 3. The relative error of prediction indicates acceptable precision, and both the limit of detection (LOD) and limit of quantification (LOQ) obtained are suitable, taking into account that a very simple methodology is applied to a complex multicomponent system.

The latter two figures of merit have been estimated using the expressions recommended by IUPAC for the detection capabilities, which take into account the so-called Type 1 and 2 errors (false detects and false non-detects, respectively) [77]. They were applied to the pseudo-univariate calibration plot (analyte scores vs. nominal concentrations) provided by MCR-ALS, as previously suggested [78].

#### 3.4. Real water samples

With the purpose of evaluating the present method in real samples and demonstrating its ability of overcoming the interference from background matrices, waters from different origins were analysed. CBZ is detected in water bodies in a wide range of concentrations, generally in the order of part- and

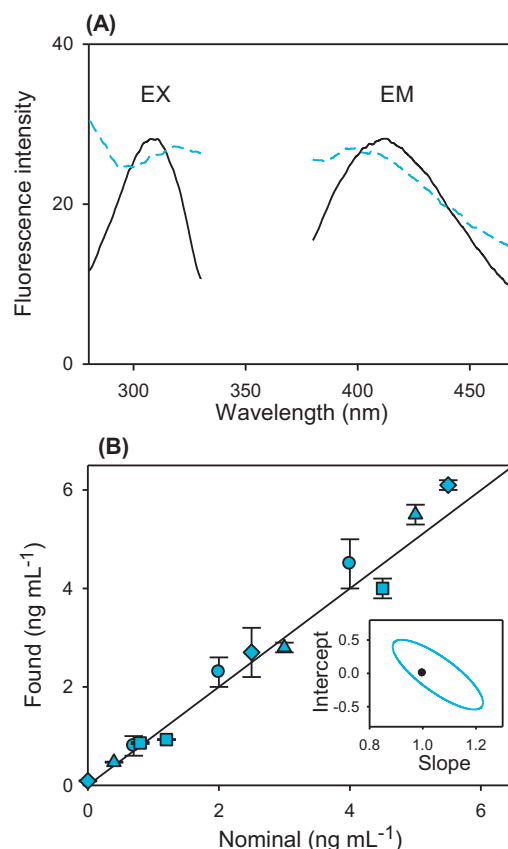


**Fig. 6.** (A) Excitation and emission fluorescence spectra of CBZ photoproducts ( $C_{CBZ} = 40.0 \text{ ng mL}^{-1}$ , black line) and background signals of a river sample without CBZ after the SPE treatment (sky-blue dashed line). (B) Plot for MCR-ALS predicted concentrations of CBZ as a function of the nominal values in a river (diamonds) and tap water (squares) samples, and in two different underground water samples (circles and triangles) spiked analyte (error bars correspond to triplicates). The inset shows the corresponding elliptical joint region at 95% confidence level. The cross marks the theoretical (intercept = 0, slope = 1) point. (For interpretation of the references to color in this figure legend, the reader is referred to the web version of this article.)

sub-part-per-billion levels. Therefore, the sensitivity of the present method was improved using a pre-concentration step by employing C18 membrane-SPE. At this point, it is necessary to point out that the selection of C18 membranes is based on our excellent experience with this solid-support as extractor of organic compounds [79–81]. Although other materials could be used for the extraction

**Table 4**

Recovery study of CBZ for spiked water samples.<sup>a</sup>

Sample	Taken (ng mL <sup>-1</sup> )	Found (ng mL <sup>-1</sup> ) <sup>b</sup>	Recovery (%)
Underground water (Funes city)	0.70	0.8 (0.2)	114
	2.00	2.3 (0.3)	115
	4.00	4.5 (0.9)	112
Underground water (Venado Tuerto city)	0.40	0.47 (0.01)	117
	3.00	2.8 (0.1)	93
	5.00	5.5 (0.2)	110
Tap water (Rosario city)	0.80	0.86 (0.02)	107
	1.20	0.93 (0.01)	78
	4.50	4.0 (0.2)	89
River water (Paraná River)	0.00	ND <sup>c</sup>	
	2.50	2.7 (0.5)	108
	5.50	6.1 (0.1)	111

<sup>a</sup> Using MCR-ALS algorithm (column-wise augmentation).

<sup>b</sup> Mean of three determinations. Standard deviations between parentheses.

<sup>c</sup> ND, not detected.

**Table 5**

Analytical performance of selected methods reported for the determination of CBZ in natural waters.

Method	VS <sup>a</sup>	Concentration level <sup>b</sup>	RSD and REC <sup>c</sup>	Sample	Refs.
SPME-GC-MS	4	LOD = 1.0	RSD = 12.0	GW, SW	[20]
SPE-GC-MS	1000	LOD = $6.5 \times 10^{-3}$ (nanopure water); LOD = $8.7 \times 10^{-3}$ (SW); 0.035–0.060 (lake); 0.030–0.250 (river); 0.100–0.800 (WWTP)	REC = 46–65 (0.100 ng mL <sup>-1</sup> )	SW, STPEs	[21]
SPE-GC-MS	1000	LOD = $9.6 \times 10^{-3}$ ; LODet = $32 \times 10^{-3}$	REC = 80 (TW) and 74 (SW)	TW, SW	[22]
SPE-HPLC-PIF	250	Without SPE: LOD = 30; LOQ = 100. With SPE: 12 (SS with 10 ng mL <sup>-1</sup> added)	RSD = 3.4	STP-WW	[23]
SPE-LC-MS/MS		STPI: 0.369. STPE: 0.426. SW (river): $0.7 \times 10^{-3}$ . SS: 0.100	REC = 83.6–103.5; RSD = 5.9	STPI, STPE, SW	[24]
SPE-GC-MS and SPE-LC-MS/MS	500–1000	MC = 1.2	Absolute REC = 89 (GC) and 99 (LC)	STPEs	[25]
SPE-GC-MS	500	LOD = 2.2; LOQ = 0.074	REC = 67	Municipal STP	[26]
SPE-LC-MS/MS		STPI: 0.356; STPE: 0.251		STPI, STPE, biosolids	[27]
SPE-GC-MS (on-line derivatization)	50–500	LOQ = $8.0 \times 10^{-3}$	REC = 79–108	TW, SW, WWE, GW	[28]
SPE-HPLC-MS	500	LOQ = $1.3 \times 10^{-3}$ (STPE); Found (STPE) = 0.033–1.3	RSD = 0.7% (10 ng per injected); RSD = 2.88 (100 ng per injected)	Urban WWs	[29]
SPE-HPLC-DAD	500–1000	WWI: LOD = 0.04; LOQ = 0.12. WWE: LOD = 0.02; LOQ = 0.06	REC = 95; RSD = 4.3	WWI, WWE	[30]
SPE-GC-MS	500	LOQ = 0.030	REC = 110; RSD = 11.5	River water	[31]
SPE-LC-MS/MS	100	LOD = 7; LOQ = 19	REC = 88.1 (1 ng mL <sup>-1</sup> ); RSD = 2.2	Hospital WWE	[32]
SPE-LC-MS/MS	100–1000	STPI: LOQ = 0.02; MC = 2. STPE: LOQ = 0.01; MC = 1.9. SW: LOQ = 0.002; MC = 0.081	Absolute REC = 36–98	STPI, STPE, SW, GW, DW	[36]
SPE (MIP)-LC-MS	100	1	REC = 80	WW	[38]
SPE-voltammetry		LOD = 9.4; LOQ = 33. SS: 500	REC = 95.8; RSD = 5.7	WW	[43]
Off- and on-line SPE-LC-QqQ-MS	500	LOD = $0.2 \times 10^{-3}$	RSD < 15	SW and DW	[15]
SPE-LDTD-APCI-MS/MS	100	0.012	RSD = 8	Municipal WW	[45]
SPE-EEPIF	10–50	LOD = 1 (PCF = 5); LOD = 0.2 (PCF = 25)	REC = 78–117; REP = 2–7	SW, UW	This work

APCI, atmospheric pressure chemical ionization; DW, drinking water; EEPID, excitation–emission photoinduced fluorimetry; GW, groundwater; LC, liquid chromatography; LTD, laser diode thermal desorption; LOD, limit of detection; LODet, limit of determination; LOQ, limit of quantification; MC, maximum found concentration; MIP, molecularly imprinted polymer; MS, mass spectrometry; MS/MS, tandem mass spectrometry; PCF, pre-concentration factor; PIF, photoinduced fluorescence; QqQ, triple quadrupole; REP, relative error of prediction; REC, recovery; RSD, relative standard deviation; SPE, solid-phase extraction; SPME, solid-phase microextraction; SS, spiked sample; STP, sewage treatment plant; STPE, sewage treatment plant effluent; STPI, sewage treatment plant influent; SW, surface water; TW, tap water; UW, underground water; VS, volume of sample; WW, wastewater; WWE, wastewater effluent; WWI, wastewater influent.

<sup>a</sup> VS, volume of sample in mL.

<sup>b</sup> For comparison, concentration units were unified to ng mL<sup>-1</sup>.

<sup>c</sup> Relative standard deviation (RSD) and recovery (REC), both in %.

procedure, previously reported experiments performed with different commercial and in-house ion-exchange polymeric sorbents were not successful for CBZ extraction [82].

Fig. 6A shows both the excitation and emission spectra of CBZ photoproducts and the signal of a typical real water sample after the SPE procedure. As can be seen, the selected sample (river water) shows intense fluorescence signals in the same region where the CBZ photoproducts emit, which are ascribed to dissolved organic matter [83]. These overlapping would preclude the direct measurement of the analyte, but it does not represent a problem when using second-order approaches. Fig. 4C shows both three-dimensional plot of the EEPID and the corresponding contour plot of real sample of river spiked with CBZ and treated with C18 membrane.

A recovery study was performed by spiking water samples with appropriate amounts of CBZ, in triplicate, at three different concentration levels, following the treatment indicated in the experimental section. According to the previous results, MCR-ALS was selected to resolve these samples, and the outstanding results obtained (Table 4, Fig. 6B) suggest that the method can overcome the problem of the presence of unexpected interferences from the background of the real samples. Table 3 displays the corresponding figures of merit obtained for these samples.

In comparison with the performances of selected methods for the determination of CBZ in natural waters (Table 5), limits of detection from  $0.2 \times 10^{-3}$  to 10 ng mL<sup>-1</sup> have been found using different strategies, all using pre-concentration procedures and most of them applying chromatographic (separation) approaches. In the present case, a low limit of detection is achieved in real samples (LOD = 0.2 ng mL<sup>-1</sup>) applying a non-sophisticated method and without using organic solvents. Note a solid-phase extraction procedure using a higher amount of sample (>50 mL) allows decrease even more the LOD. Additionally, a sampling rate of about six samples per hour (including the EEPID measuring) makes the method very advantageous.

#### 4. Conclusions

A novel and simple fluorimetric method for carbamazepine (CBZ) determination was developed and successfully applied to the quantitation of this emerging contaminant in water samples. Analyses were accomplished in a significant short time, with a minimum operator effort and avoiding the use of organic solvents. The selectivity of the method is achieved through the coupling of multivariate calibration. Among the different second-order

algorithms investigated, multivariate curve resolution-alternating least-squares (MCR-ALS) showed a superior predictive capability and would be the recommended one in situations where interferences present similar profiles as the investigated compound.

## Acknowledgments

The authors gratefully acknowledge Universidad Nacional de Rosario and Consejo Nacional de Investigaciones Científicas y Técnicas (Project PIP 1950) for financially supporting this work.

## Appendix A. Supplementary data

Supplementary data associated with this article can be found, in the online version, at <http://dx.doi.org/10.1016/j.aca.2013.04.020>.

## References

- [1] A. Goodman Gilman, J.G. Hardman, L.E. Limbird, Goodman & Gilman's *the Pharmacological Basis of Therapeutics*, 10th ed., Mc-Graw Hill, New York, 2001.
- [2] S.D. Richardson, T.A. Ternes, *Anal. Chem.* 83 (2011) 4614.
- [3] M. Schriks, M.B. Heringa, M.M.E. van der Kooi, P. de Voogt, A. van Wezel, *Water Res.* 44 (2010) 461.
- [4] V.L. Cunningham, C. Perino, V.J. D'Aco, A. Hartmann, R. Bechter, *Regul. Toxicol. Pharm.* 56 (2010) 343.
- [5] S. Madden, J.L. Maggs, B.K. Park, *Drug Metab. Dispos.* 24 (1996) 469.
- [6] R. Andreozzi, R. Marotta, G. Pinto, A. Pollio, *Water Res.* 36 (2002) 2869.
- [7] S. Chiron, C. Minero, D. Vione, *Environ. Sci. Technol.* 40 (2006) 5977.
- [8] T. Kosiek, H.R. Andersen, B. Kompare, A. Ledin, E. Heath, *Environ. Sci. Technol.* 43 (2009) 6256.
- [9] M. Gros, M. Petrović, D. Barceló, *Anal. Bioanal. Chem.* 386 (2006) 941.
- [10] M. Petrović, D. Barceló, *Trends Anal. Chem.* 26 (2007) 486.
- [11] C. Tixier, H.P. Singer, S. Oellers, S.R. Müller, *Environ. Sci. Technol.* 37 (2003) 1061.
- [12] R. Loos, B.M. Gawlik, G. Locoro, E. Rimaviciute, S. Contini, G. Bidoglio, *Environ. Pollut.* 157 (2009) 561.
- [13] R. Loos, G. Locoro, S. Comero, S. Contini, D. Schwesig, F. Werres, P. Balsaa, O. Gans, S. Weiss, L. Blaha, M. Bolchi, B.M. Gawlik, *Water Res.* 44 (2010) 4115.
- [14] M. Clara, B. Strenn, N. Kreuzinger, *Water Res.* 38 (2004) 947.
- [15] P.A. Segura, S.L. MacLeod, P. Lemoine, S. Sauvè, C. Gagnon, *Chemosphere* 84 (2011) 1085.
- [16] J. Wang, P.R. Gardinali, *Anal. Bioanal. Chem.* 404 (2012) 2711.
- [17] M. Furlanet, M.G. Delucca, G. Dilberis, A. Barnaba, *Br. J. Clin. Pharmacol.* 11 (1981) 393.
- [18] J.L. Maggs, M. Pirmohamed, N.R. Kitteringham, B.K. Park, *Drug Metab. Dispos.* 25 (1997) 275.
- [19] G.F. van Rooyen, D. Badenhorst, K.J. Swart, H.K.L. Hundt, T. Scanes, A.F. Hundt, *J. Chromatogr. B* 769 (2002) 1.
- [20] M. Moeder, S. Schrader, M. Winkler, P. Popp, *J. Chromatogr. A* 873 (2000) 95.
- [21] S. Öllers, H. Singer, P. Fässler, *J. Chromatogr. A* 911 (2001) 225.
- [22] F. Sacher, F. Lange, H. Brauch, I. Blankenhorn, *J. Chromatogr. A* 938 (2001) 199.
- [23] C. González Barreiro, M. Lores, M.C. Casais, R. Cela, *J. Chromatogr. A* 993 (2003) 29.
- [24] X.S. Miao, C.D. Metcalfe, *Anal. Chem.* 75 (2003) 3731.
- [25] R. Andreozzi, M. Raffaele, P. Nicklas, *Chemosphere* 50 (2003) 1319.
- [26] M. Carballa, F. Omil, J.M. Lema, M. Llompart, C. García Jares, I. Rodríguez, M. Gómez, T. Ternes, *Water Res.* 38 (2004) 2918.
- [27] X.S. Miao, J.J. Yang, C.D. Metcalfe, *Environ. Sci. Technol.* 39 (2005) 7469.
- [28] W.C. Lin, H.C. Chen, W.H. Ding, *J. Chromatogr. A* 1065 (2005) 279.
- [29] S. Castiglioni, R. Bagnati, D. Calamari, R. Fanelli, E. Zuccato, *J. Chromatogr. A* 1092 (2005) 206.
- [30] J.L. Santos, I. Aparicio, E. Alonso, M. Callejón, *Anal. Chim. Acta* 550 (2005) 116.
- [31] Z. Moldovan, *Chemosphere* 64 (2006) 1808.
- [32] M.J. Gómez, M. Petrović, A.R. Fernández Alba, D. Barceló, *J. Chromatogr. A* 1114 (2006) 224.
- [33] M.R. Hadjimohammadi, P. Ebrahimi, *Anal. Chim. Acta* 516 (2004) 141.
- [34] H. Breton, M. Cociglio, F. Bressolle, H. Peyriere, J.P. Blayac, D. Hillaire Buys, *J. Chromatogr. B* 828 (2005) 80.
- [35] T. Yoshida, K. Imai, S. Motohashi, S. Hamano, M. Sato, *J. Pharm. Biomed. Anal.* 41 (2006) 1386.
- [36] D. Hummel, D. Löfller, G. Fink, T.A. Ternes, *Environ. Sci. Technol.* 40 (2006) 7321.
- [37] D. Fatta, A. Nikolaou, A. Achilleos, S. Meriç, *Trends Anal. Chem.* 26 (2007) 515.
- [38] A. Beltran, E. Caro, R.M. Marcé, P.A.G. Cormack, D.C. Sherrington, F. Borrull, *Anal. Chim. Acta* 597 (2007) 6.
- [39] S. Wu, W. Xu, Q. Subhani, B. Yang, D. Chen, Y. Zhu, L. Li, *Talanta* 101 (2012) 541.
- [40] Z. Rezaei, B. Hemmateenejad, S. Khabnadideh, M. Gorgin, *Talanta* 65 (2005) 21.
- [41] B. Hemmateenejad, Z. Rezaei, S. Khabnadideh, M. Saffari, *Spectrochim. Acta A* 68 (2007) 718.
- [42] M.S. Cámaras, C. Mastandrea, H.C. Goicoechea, *J. Biochem. Biophys. Methods* 64 (2005) 153.
- [43] A. Veiga, A. Dordio, A.J. Palace Carvalho, D. Martins Teixeira, J. Ginja Teixeira, *Anal. Chim. Acta* 674 (2010) 182.
- [44] B. Unnikrishnan, V. Mani, S.M. Chen, *Sens. Actuators B* 173 (2012) 274.
- [45] D.P. Mohapatra, S.K. Brar, R.D. Tyagi, P. Picard, R.Y. Surampalli, *Talanta* 99 (2012) 247.
- [46] L. Vera Candioti, M.J. Culzoni, A.C. Olivieri, H.C. Goicoechea, *Electrophoresis* 29 (2008) 4527.
- [47] Y.Y. Lin, C.C. Wang, Y.H. Ho, C.S. Chen, S.M. Wu, *Anal. Bioanal. Chem.* 405 (2013) 259.
- [48] G.M. Escandar, D. González Gómez, A. Espinosa Mansilla, A. Muñoz de la Peña, H.C. Goicoechea, *Anal. Chim. Acta* 506 (2004) 161.
- [49] S. Kuhn, N. Meier, O. Pierart, G. Godoy, *Farmaco Ed. Prat.* 37 (1982) 296.
- [50] L. De la Peña, A. Gomez Hens, D. Pérez Bendito, *Fresenius J. Anal. Chem.* 338 (1990) 821.
- [51] Z.T. Pan, L.F. Yao, Chin. J. Anal. Chem. 26 (1998) 997.
- [52] Z.Q. Zhang, G.X. Liang, J. Ma, *Anal. Lett.* 39 (2006) 2417.
- [53] C. Huang, Q. He, H. Chen, *J. Pharm. Biomed. Anal.* 30 (2002) 59.
- [54] P. Anastas, N. Eghbali, *Chem. Soc. Rev.* 39 (2010) 301.
- [55] J.A. Linthorst, *Found Chem.* 12 (2010) 55.
- [56] R. Bro, *Chemometr. Intell. Lab. Syst.* 38 (1997) 149.
- [57] J. öhman, P. Geladi, S. Wold, *J. Chemometr.* 4 (1990) 135.
- [58] A.C. Olivieri, *J. Chemometr.* 19 (2005) 253.
- [59] R. Bro, *J. Chemometr.* 10 (1996) 47.
- [60] R. Tauler, *Chemometr. Intell. Lab. Syst.* 30 (1995) 133.
- [61] K.S. Booksh, B.R. Kowalski, *Anal. Chem.* 66 (1994) 782A.
- [62] A. Rinnan, J. Riu, R.J. Bro, *J. Chemometr.* 21 (2007) 76.
- [63] MATLAB R2011b, The MathWorks Inc., Natick, MA, USA.
- [64] V. Calisto, M.R.M. Domingues, G.L. Erny, V.I. Esteves, *Water Res.* 45 (2011) 1095.
- [65] D. Vogna, R. Marotta, R. Andreozzi, A. Napolitano, M. d'Ischia, *Chemosphere* 54 (2004) 497.
- [66] A.M. García Campaña, J.J. Aaron, J.M. Bosque Sendra, *Talanta* 55 (2001) 531.
- [67] E.M. Almansa Lopez, A.M. García Campaña, J.J. Aaron, L. Cuadros Rodríguez, *Talanta* 60 (2003) 355.
- [68] M. Stuart, D. Lapworth, E. Crane, A. Hart, *Sci. Total Environ.* 416 (2012) 1.
- [69] R. Bro, H.L. Kiers, *J. Chemometr.* 17 (2003) 274.
- [70] P.C. Damiani, I. Durán Merás, A. García Reiriz, A. Jiménez Jirón, A. Muñoz de la Peña, A.C. Olivieri, *Anal. Chem.* 79 (2007) 6949.
- [71] A.C. Olivieri, G.M. Escandar, A. Muñoz de la Peña, *Trends Anal. Chem.* 30 (2011) 607.
- [72] A.G. González, M.A. Herrador, A.G. Asuero, *Talanta* 48 (1999) 729.
- [73] D.M. Haaland, E.V. Thomas, *Anal. Chem.* 60 (1988) 1193.
- [74] S.A. Bortolato, J.A. Arancibia, G.M. Escandar, *Anal. Chem.* 80 (2008) 8276.
- [75] W. Windig, J. Guilment, *Anal. Chem.* 63 (1991) 1425.
- [76] J. Kuligowski, G. Quintas, R. Tauler, B. Lendl, M. de la Guardia, *Anal. Chem.* 83 (2011) 4855.
- [77] L.A. Currie, *Anal. Chim. Acta* 391 (1999) 127.
- [78] J. Saurina, C. Leal, R. Compañó, M. Granados, M.D. Prat, R. Tauler, *Anal. Chim. Acta* 432 (2001) 241.
- [79] G.N. Piccirilli, G.M. Escandar, F. Cañada Cañada, I. Durán Merás, A. Muñoz de la Peña, *Talanta* 77 (2008) 852.
- [80] S.A. Bortolato, J.A. Arancibia, G.M. Escandar, *Anal. Chem.* 81 (2009) 8074.
- [81] M. Bravo, L.F. Aguilar, W. Quiroz, A.C. Olivieri, G.M. Escandar, *Microchem. J.* 106 (2013) 95.
- [82] D. Bratkowska, R.M. Marcé, P.A.G. Cormack, D.C. Sherrington, F. Borrull, N. Fontanals, *J. Chromatogr. A* 1217 (2010) 1575.
- [83] N. Hudson, A. Baker, D. Reynolds, *River Res. Appl.* 23 (2007) 631.